

## Research Article

# miRNAs from Plasma Extracellular Vesicles Are Signatory Noninvasive Prognostic Biomarkers against Atherosclerosis in LDLr<sup>-/-</sup> Mice

Ke-feng Zhai <sup>1,2,3,4</sup> Hong Duan <sup>2</sup> Yan Shi,<sup>2</sup> Ya-ru Zhou,<sup>2</sup> Yuan Chen,<sup>2</sup> Yao-shuai Zhang,<sup>5</sup> Zi-peng Gong <sup>4</sup> Wen-gen Cao,<sup>2</sup> Jia Wu,<sup>1</sup> and Jun-jun Wang <sup>1</sup>

<sup>1</sup>Department of Clinical Laboratory, Jinling Hospital, Medical School of Nanjing University, Nanjing 210002, China

<sup>2</sup>Suzhou Engineering and Technological Research Center of Natural Medicine and Functional Food, School of Biological and Food Engineering, Suzhou University, 49, Bianhe Road, Suzhou 234000, China

<sup>3</sup>State Key Laboratory for Chemistry and Molecular Engineering of Medicinal Resources (Guangxi Normal University), Guilin 541004, China

<sup>4</sup>State Key Laboratory of Functions and Applications of Medicinal Plants, Guizhou Provincial Key Laboratory of Pharmaceutics, Engineering Research Center for the Development and Application of Ethnic Medicine and TCM (Ministry of Education), Guizhou Medical University, Guiyang 550004, China

<sup>5</sup>Faculty of Pharmacy, Bengbu Medical College, Bengbu 233030, China

Correspondence should be addressed to Hong Duan; [szxydh@163.com](mailto:szxydh@163.com), Zi-peng Gong; [gzp4012607@126.com](mailto:gzp4012607@126.com), and Jun-jun Wang; [wangjunjun9202@163.com](mailto:wangjunjun9202@163.com)

Received 24 February 2022; Revised 15 July 2022; Accepted 20 July 2022; Published 17 August 2022

Academic Editor: Gabriele Saretzki

Copyright © 2022 Ke-feng Zhai et al. This is an open access article distributed under the Creative Commons Attribution License, which permits unrestricted use, distribution, and reproduction in any medium, provided the original work is properly cited.

Circular microRNAs (miRNAs) have become central in pathophysiological conditions of atherosclerosis (AS). However, the biomarkers for diagnosis and therapeutics against AS are still unclear. The atherosclerosis models in low-density lipoprotein receptor deficiency (LDLr<sup>-/-</sup>) mice were established with a high-fat diet (HFD). The extraction kit isolated extracellular vesicles from plasma. Total RNAs were extracted from LDLr<sup>-/-</sup> mice in plasma extracellular vesicles. Significantly varying miRNAs were detected by employing Illumina HiSeq 2000 deep sequencing technology. Target gene predictions of miRNAs were employed by related software that include RNAhybrid, TargetScan, miRanda, and PITA. Gene Ontology (GO) and Kyoto Encyclopedia of Genes and Genomes (KEGG) further analyzed the intersection points of predicted results. The results showed that the HFD group gradually formed atherosclerotic plaques in thoracic aorta compared with the control group. Out of 17, 8 upregulated and 9 downregulated miRNAs with a significant difference were found in the plasma extracellular vesicles that were further cross-examined by sequencing and bioinformatics analysis. Focal adhesion and Ras signaling pathway were found to be the most closely related pathways through GO and KEGG pathway analyses. The 8 most differentially expressed up- and downregulated miRNAs were further ascertained by TaqMan-based qRT-PCR. TaqMan-based qRT-PCR and in situ hybridization further validated the most differentially expressed miRNAs (miR-378d, miR-181b-5p, miR-146a-5p, miR-421-3p, miR-350-3p, and miR-184-3p) that were consistent with deep sequencing analysis suggesting a promising potential of utility to serve as diagnostic biomarkers against AS. The study gives a comprehensive profile of circular miRNAs in atherosclerosis and may pave the way for identifying biomarkers and novel targets for atherosclerosis.

## 1. Introduction

In the early nineties, microRNAs (miRNAs) were first discovered in *Caen Elegans*. The miRNA is a single-strand, endogenous, nonprotein-coding small RNA molecule of about 22 nucleotides [1]. The miRNAs have particular roles in gene regulation at the posttranscriptional level [2, 3]. The miRNA can discern the corresponding region of specific target mRNA and then interact with it, leading to mRNA degradation or expression suppression [4]. To date, almost 721 human and 579 mouse miRNAs have been affirmed, which regulate about 30% of protein-coding genes in human beings. One miRNA can control no less than one target gene, and multiple miRNAs can regulate the target genes. The modulations in miRNAs are associated with the development and progression of several diseases, such as atherosclerosis (AS), nasopharyngeal carcinoma (NPC), obesity, and diabetes [5–7]. Therefore, the miRNAs might be used as biomarkers in these diseases.

The most prevailing cause of coronary heart disease, cerebral infarction, and peripheral vascular disease is atherosclerosis, where the obstacle of lipid metabolism is the basis of atherosclerosis [8]. This chronic inflammatory disease is caused by the aggression of WBCs to the oxidized low-density lipoproteins (LDL) with the recruitment of activated endothelial cells (ECs) [9]. Atherosclerosis is characterized by increased oxidative stress associated with endothelial dysfunction, infiltration of leukocytes, and deposition of modified lipoproteins [10]. The harmful consequence of oxidized LDL further accumulates the cytokine secretions, growth factors, and leukocytes that collectively accelerate the lesion and inflammation that ultimately end up to atherosclerosis [5].

Presently, major clinical diagnostic methods of atherosclerosis include biochemical examination, blood profiling with a particular focus on lipids, and X-ray examination; however, there are still many niches in early and accurate diagnosis of atherosclerosis. The miRNA-based gene regulations are already in practice for diagnosing many diseases [11, 12]. Our present study was designed to detect miRNAs from extracellular vesicles (EVs) in plasma by high-throughput RNA sequencing that may serve as targets for further exploration on miRNA-based diagnostic tool against AS.

## 2. Material and Methods

**2.1. Animals and Atherosclerosis Model.** Low-density lipoprotein receptor (LDLr) deficiency male C57BL/6 mice (8 weeks old,  $18 \pm 2$  g body weight) were obtained from Model Animal Research Center, Nanjing, China. The animals were kept at standard temperature  $22 \pm 2^\circ\text{C}$ , with air conditioning and relative humidity of 55%–65% with 12 h light/12 h dark circulation. LDLr<sup>-/-</sup> mice were divided into the control and high-fat diet (HFD) groups, with eight mice in each group. The mice in the HFD group were induced with atherosclerosis through a 12-week high-fat diet (LDLr<sup>-/-</sup> mice were fed a high-fat diet containing 21% fat and 0.21% cholesterol (D12079B, Open Source Diets, Research Diets, Inc.)) [13–15]; in contrast, the mice in the control group were given a normal feed (LDLr<sup>-/-</sup> mice were fed a standardized chow diet). The drinking water of the mice was disinfected by ultraviolet light, and the water

bottle and the pad material were changed every other day. All animal handling processes complied with the application of the guidelines for experimental animal care of Suzhou University (SZU-19002).

**2.2. Hematoxylin and Eosin (HE) Staining.** The mice were anesthetized with pentobarbital sodium and fixed on the dissecting table to expose the chest cavity. The base of the ascending aorta and the brachial artery were separated after perfusion of the left ventricle with cold PBS and cold 4% paraformaldehyde. The aortic root was cut into  $5\ \mu\text{m}$  sections, and paraffin was removed after paraffin embedding. HE staining was carried out finally after rehydration.

**2.3. Isolation and Detection of Extracellular Vesicles.** All mice were sacrificed and blood from both groups' mice were collected, centrifuged, and preserved for further analyses as described in earlier studies [16]. Blood samples were collected in EDTA blood tubes and centrifuged to separate the plasma fraction. Plasma samples were then stored at  $-80^\circ\text{C}$  until further processing.

The exoEasy Maxi kit (Qiagen, 76064) was used to extract extracellular vesicles (EVs) from plasma according to manufacturer instructions [17]. The extracellular vesicle morphology was determined by a transmission electron microscope (TEM; JEM-1200EX, Japan) with a protocol modification as described by Rodriguez-Caro and Dragovic [18]. Briefly,  $10\ \mu\text{L}$  of EVs was loaded onto Cu grids and incubated for 10 min at room temperature. They were then stained with 2% uranyl acetate (aqueous) for 2 min before air drying and examination by TEM. The sizes of the EVs were analyzed by nanoparticle tracking analysis (NTA) using a Zetaview (Particle Metrix) with a 488 nm laser [17]. All EV samples were diluted in PBS for 100 times before NTA and then analyzed according to manufacturer instructions. In addition, the presence of specific EV markers was determined by western blot. Briefly, isolated EVs were nurtured with lysis buffer. After resolving the protein samples (30 mg) on SDS-polyacrylamide gelelectrophoresis (SDS-PAGE), they were shifted to polyvinylidene difluoride (PVDF) films. The loaded membranes were blocked with 5% skimmed milk and incubated with primary antibodies (Cell Signaling Technology, Beverly, MA, USA) and secondary antibodies (Bioworld Technology Inc, St. Louis Park, MN, USA) for overnight at  $4^\circ\text{C}$  and 2 h at room temperature, respectively. Immunoreactive protein bands and their intensities were visualized under the FluorChem HD2 Imaging system (Protein Simple, CA, USA) and Alpha View SA, respectively [19].

**2.4. RNA Extraction.** Total extracellular vesicle RNAs were extracted by Express miRNA Extraction Kit (Tissue and cell). After thawing the plasma, it was stored on ice for later use. The plasma was centrifuged at  $2000\ \text{g}$  and  $4^\circ\text{C}$  for 20 min for 20 min. The clear supernatant was taken to the new EP tube and then centrifuged at  $10000\ \text{g}$  and  $4^\circ\text{C}$  for 20 min, and again, a clear supernatant was shifted to the new EP tube. It was then added with  $75\ \mu\text{L}$  PBS and mixed evenly, afterwards, and  $7.5\ \mu\text{L}$  proteinase K was mixed with the sample and incubated for 10 min at  $37^\circ\text{C}$ . Then, it was added with  $45\ \mu\text{L}$  outside secrete body sedimentation reagent (total extracellular vesicles

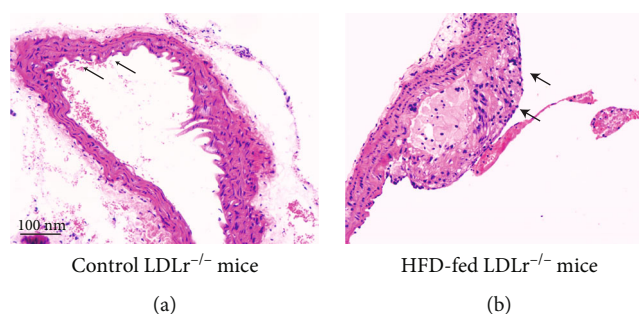


FIGURE 1: Assessment of the atherosclerotic status in LDLr<sup>-/-</sup> mice. (a) Control group. (b) High-fat diet- (HFD-) fed group. Representative HE stains of aortic coronal vessel section ( $\times 200$ ), scale bar 100 nm,  $n = 8$ .

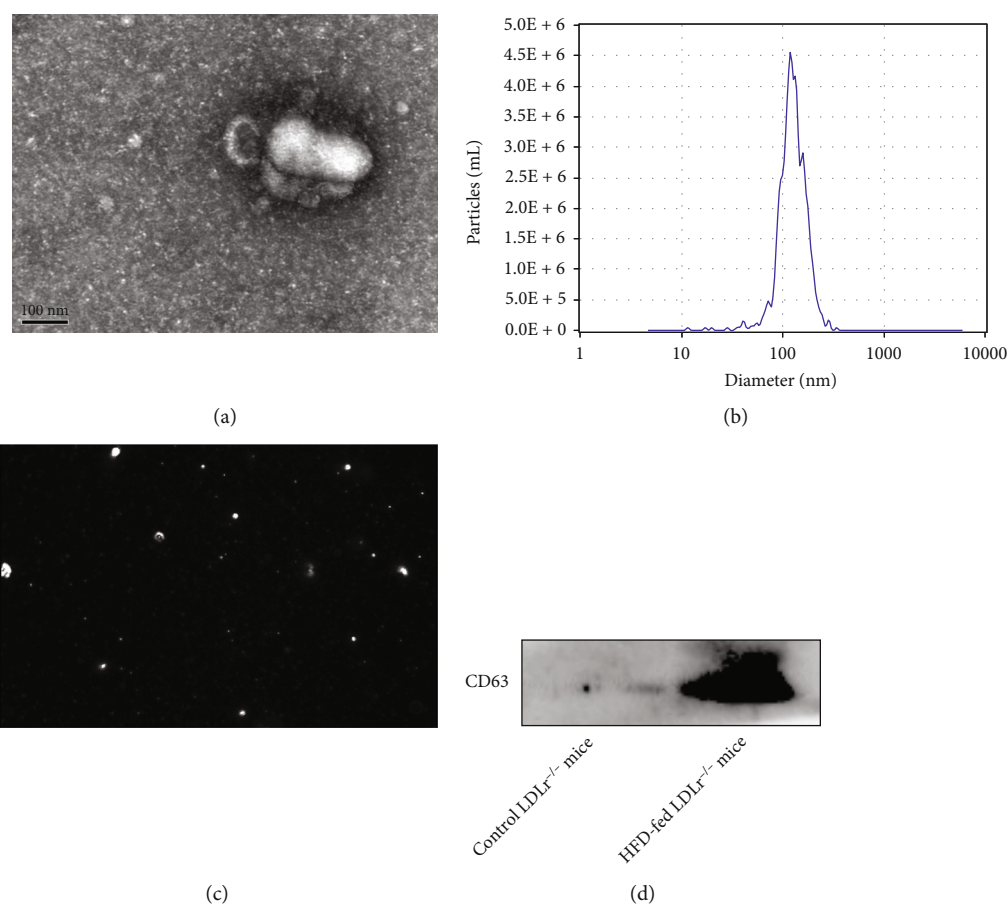


FIGURE 2: Detection of extracellular vesicles. (a) Representative TEM image of extracellular vesicles (scale bar 100 nm),  $n = 8$ . (b) Nanoparticle tracking analysis (NTA) of extracellular vesicles. (c) Video capture of recorded extracellular vesicle movements. (d) Standard markers CD63 was detected by western blot.

isolation (from plasma)) and mixed at 4°C after incubation for 30 min. After the incubation of 30 min, the mixed solution was centrifuged at 10000 g and 4°C for 30 min. After centrifugation for 30 min, 50  $\mu$ L PBS was added to the supernatant and resuspended. Out of this prepared solution of microRNA, 300  $\mu$ L microRNA and Reagent A were mixed and allowed to settle for 5 min at room temperature and then mixed with Reagent B. The solution was centrifuged at 13000 g for 5 min at a low temperature (not higher than 4°C). Out of this solution,

550  $\mu$ L of the supernatant was shifted from this solution to a new EP tube containing 200  $\mu$ L of absolute ethanol. The mixture was left at room temperature for five minutes and then centrifuged under the same conditions for ten minutes. Then, moved 700  $\mu$ L to a new EP supernatant fluid tube and added 300  $\mu$ L isopropanol and blended. Two solutions in EP tubes were transferred to the adsorption column for centrifugation at 13000 g at 4°C for 1 min and abandoned the supernatant. Isopropanol (75%) for 700  $\mu$ L was added to the adsorption

TABLE 1: Differentially expressed miRNAs from different groups ( $n = 8$ ).

sRNA id	Count (control)	Count (model)	TPM (control)	TPM (model)	log2 ratio (model/control)	Up-downregulation (model/control)	$p$ value	FDR
mmu-miR-378d	13	2165	1	168	7.3939481	Up	0	0
mmu-miR-181b-5p	103	10108	7.93	785	6.6297057	Up	0	0
mmu-miR-107-3p	199	1781	15.3	138	3.1749387	Up	0	0
mmu-miR-146a-5p	269	1039	20.7	80.7	1.9625986	Up	$1.20E-108$	$3.64E-107$
novel_mir20	19	61	1.46	4.74	1.6989187	Up	$1.46E-06$	$1.35E-05$
mmu-miR-8112	43	138	3.31	10.7	1.6954018	Up	$3.46E-13$	$4.16E-12$
mmu-miR-122-5p	271	658	20.9	51.1	1.2924572	Up	$9.65E-39$	$1.80E-37$
mmu-miR-9b-3p	156	346	12	26.9	1.162297	Up	$4.14E-18$	$5.50E-17$
mmu-miR-421-3p	4063	1918	313	149	-1.070159	Down	$6.06E-169$	$2.13E-167$
mmu-miR-350-3p	795	338	61.2	26.3	-1.2209	Down	$3.14E-42$	$6.27E-41$
mmu-miR-184-3p	412	174	31.7	13.5	-1.230298	Down	$6.27E-23$	$9.02E-22$
mmu-miR-331-3p	78	25	6.01	1.94	-1.631308	Down	$1.34E-07$	$1.31E-06$
mmu-miR-700-3p	48	13	3.7	1.01	-1.87317	Down	$5.67E-06$	$4.97E-05$
mmu-miR-6538	56	11	4.31	0.85	-2.342153	Down	$1.57E-08$	$1.62E-07$
novel_miR10	17	0	1.31	0	-10.35535	Down	$8.26E-06$	$7.04E-05$
novel_miR18	30	0	2.31	0	-11.17368	Down	$1.07E-09$	$1.14E-08$
novel_miR23	78	0	6.01	0	-12.55315	Down	$4.70E-24$	$7.11E-23$

column, which then was centrifuged at 13000g at 4°C for 1 min, and the supernatant was discarded. Adding 500  $\mu$ L of anhydrous ethanol to the adsorption column was centrifuged under the same conditions, and the supernatant was discarded. RNase-free TE buffer was added to the adsorption column filter and then allowed to settle for 2 min. After centrifugation, the product of extracted miRNAs was obtained by elution with eluent.

**2.5. Screening Significant Differential miRNAs.** Total RNA was extracted from the plasma of two groups of mice. HiSeq 2000 deep sequencing technology (Shenzhen BGI Co. Ltd., Wuhan, China) was applied to screen out the miRNAs with significant differences in expression [20, 21]. The false discovery rate (FDR) was indicated as the multiple difference between the control and model groups. The fold change (FC) and  $p$  values were calculated by applying the Student  $t$ -test [22].

**2.6. Bioinformatics Analysis.** Multiple bioinformatics software (TargetScan, miRanda, and RNAhybrid) were employed to predict differentially expressed miRNA targets [23]. After appropriate statistical analyses (formula) with a  $p$  value of less than 0.05, the common regions obtained from three software were further subjected to the KEGG and GO enrichment analyses [24].

Formula:

$$P = 1 - \sum_{i=0}^{m-1} \frac{\binom{M}{i} \binom{N-M}{n-i}}{\binom{N}{n}}. \quad (1)$$

**2.7. Confirmation of Expression of miRNAs.** After a shortlisting of differentially expressed miRNAs through deep sequencing and bioinformatics software, the atherosclerosis-related miRNAs were further subjected to TaqMan-based qRT-PCR analyses to confirm diagnostic biomarkers as described earlier [25, 26]. The miRNAs were obtained from extracellular vesicles in plasma using Express miRNA Extraction Kit (Tissue and cell). All-in-One First-Strand cDNA Synthesis kit (Haigene Biotech, Haerbin, China) was used for reverse transcription for total RNAs using U6 snRNA as an internal reference gene [27, 28]. All samples were normalized to internal control, and fold changes were calculated through relative quantification.

**2.8. In Situ Hybridization.** In situ hybridization was performed as described previously [29]. The sections (5  $\mu$ m thick) were subjected to in situ hybridization kit (Exiqon, BOSTER Biological Technology Co. Ltd., China) following the manufacturer's instructions. DAPI was used as a nuclear counterstain. Slides were visualized using a confocal microscope (Olympus, Tokyo, Japan).

### 3. Results

**3.1. Atherosclerosis Formation in LDLr<sup>-/-</sup> Mice.** To study the formation of atherosclerosis *in vivo*, the plaque area and plaque composition in aortic roots were assessed by histopathological analyses. As shown in Figure 1, the LDLr<sup>-/-</sup> mice treated with a high-fat diet (model group) displayed the most favorable plaque phenotype. The plaque and lesions were significantly larger than the control group, indicating that atherosclerosis developed successfully.

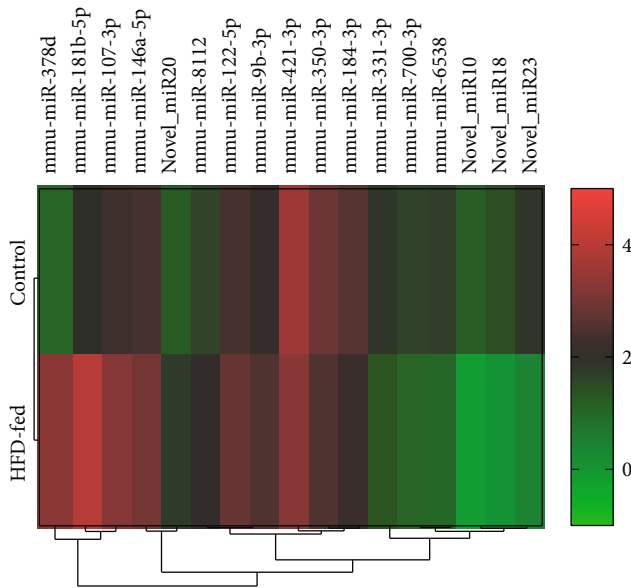


FIGURE 3: Heatmap of normalized miRNA reads that are differentially expressed between the control and HFD-fed groups,  $n = 8$ .

**3.2. Extracellular Vesicle Detection.** TEM analysis revealed that the extracellular vesicles from the plasma were irregular circular or elliptic structures with diameters of 30–200 nm. At the same time, the vesicles were observed to have a complete enveloped membrane (Figure 2(a)). Furthermore, we used NTA to determine the size and concentration of extracellular vesicles. As shown (Figures 2(b) and 2(c)), the diameters of plasma extracellular vesicles were 50 nm to 200 nm. The concentration of extracellular vesicles was  $7.7 \times 10^{10}$  particles/mL. Moreover, specific EV markers CD63 was perceived by western blot (Figure 1(d)). A large amount of CD63 was detected in the HFD-fed LDLr<sup>-/-</sup> mice group in western blot experiment, indicating that a large amount of EVs was secreted in the HFD-fed LDLr<sup>-/-</sup> mice group. The above experimental results showed that we had extracted and isolated good secretory EVs from plasma.

**3.3. Classification of miRNAs.** MicroRNA annotation statistics were identified by comparing them with the known sRNA database. To make each unique miRNA have a unique annotation, miRNAs were traversed and annotated according to the priority order of miRNA > pi-RNA > snoRNA > R-fam > others RNA [2, 30]. The information on mature and progeny miRNA was obtained by comparing the classification of annotation results and earlier reported database of mature miRNA. With the comparison of the miRNA database, some of the unknown (experimentally found) miRNAs were identified (Supplementary Table 1), while some other remaining unknown miRNAs were considered novel miRNAs. Thus, we have predicted some new miRNAs with the sequencing process (Supplementary Table 2).

**3.4. Differentially Expressed miRNAs from Different Groups.** Multiple software predicted the target genes of miRNAs with significant differences of expressions. In general, the miR-

NAs with a significant difference in an expression whose FDR was less than or equal to 0.001 and the multiple difference of it was more than two times were screened out. A total of 17 miRNAs showed a significant difference in expressions. Nine downregulated miRNAs (miR-421-3p, miR-350-3p, miR-184-3p, miR-331-3p, miR-700-3p, miR-6538, novel\_miR10, novel\_miR18, and novel\_miR23), and 8 upregulated miRNAs (miR-378d, miR-181b-5p, miR-107-3p, miR-146a-5p, miR-122-5p, miR-8112, miR-9b-3p, and novel\_miR20) were found and listed (Table 1).

Heatmap in R software was applied to hierarchical clustering analysis (Figure 3). Collectively, the normal mice and LDLr<sup>-/-</sup> mice were correctly separated because of 17 differentially expressed miRNAs by the clustering analysis (Figure 3). Therefore, these 17 miRNAs have the strong potential for their utility to detect atherosclerotic lesions.

**3.5. Target Gene Prediction and Functional Analysis of miRNAs.** Multiple bioinformatics software (TargetScan, PITA, miRanda, and RNAhybrid) were employed to predict differentially expressed miRNA target genes. The common intersecting regions from this four software indicated of 17 differentially expressed miRNAs (Supplementary Table 3). After appropriate statistical analyses and normalization for a  $p$  value of less than 0.05, the common regions obtained from these four software were further subjected to the GO significance enrichment analysis. The key functions incorporated for analysis included cellular components (CC), biological processes (BP), and molecular function (MF). GO function significance enrichment analysis was beneficial for determining the major biological functions of target genes of the differentially expressed sRNAs. These functioning entries in GO indicated the target genes' biological functions corresponding to the differentially expressed miRNA and their signal correlation. The results indicated that the differentially expressed genes were focused on cell periphery (Figure 4(a)), protein binding (Figure 4(b)), and regulation of signaling (Figure 4(c)), respectively.

To further comprehend the biological functions and their corresponding pathways, KEGG was employed using single unit function. The hypergeometric test was assessed for the differentially expressed miRNAs target genes compared with the whole genome background. The top 20 pathways are shown in Figure 5. Focal adhesion and Ras signaling pathways were found to be strongly associated with AS. The KEGG classification counts the number and composition of proteins and genes (Figure 6). The results indicated cell progression and death; signal transduction against environmental factors; gene folding, sorting, and degradation; lipid metabolism; and circulatory and cardiovascular system may be closely connected with AS.

**3.6. Validation of Expression of miRNAs.** As 17 differentially expressed miRNAs were attained from deep sequencing to obtain the most exact diagnostic biomarker of AS, the top 8 miRNAs (4 upregulated and 4 downregulated miRNAs) were assessed by TaqMan-based qRT-PCR. The relative levels of each miRNA were obtained and shown in Figure 7(a). mmu-miR-378d, mmu-miR-181b-5p, and mmu-miR-146a-5p in

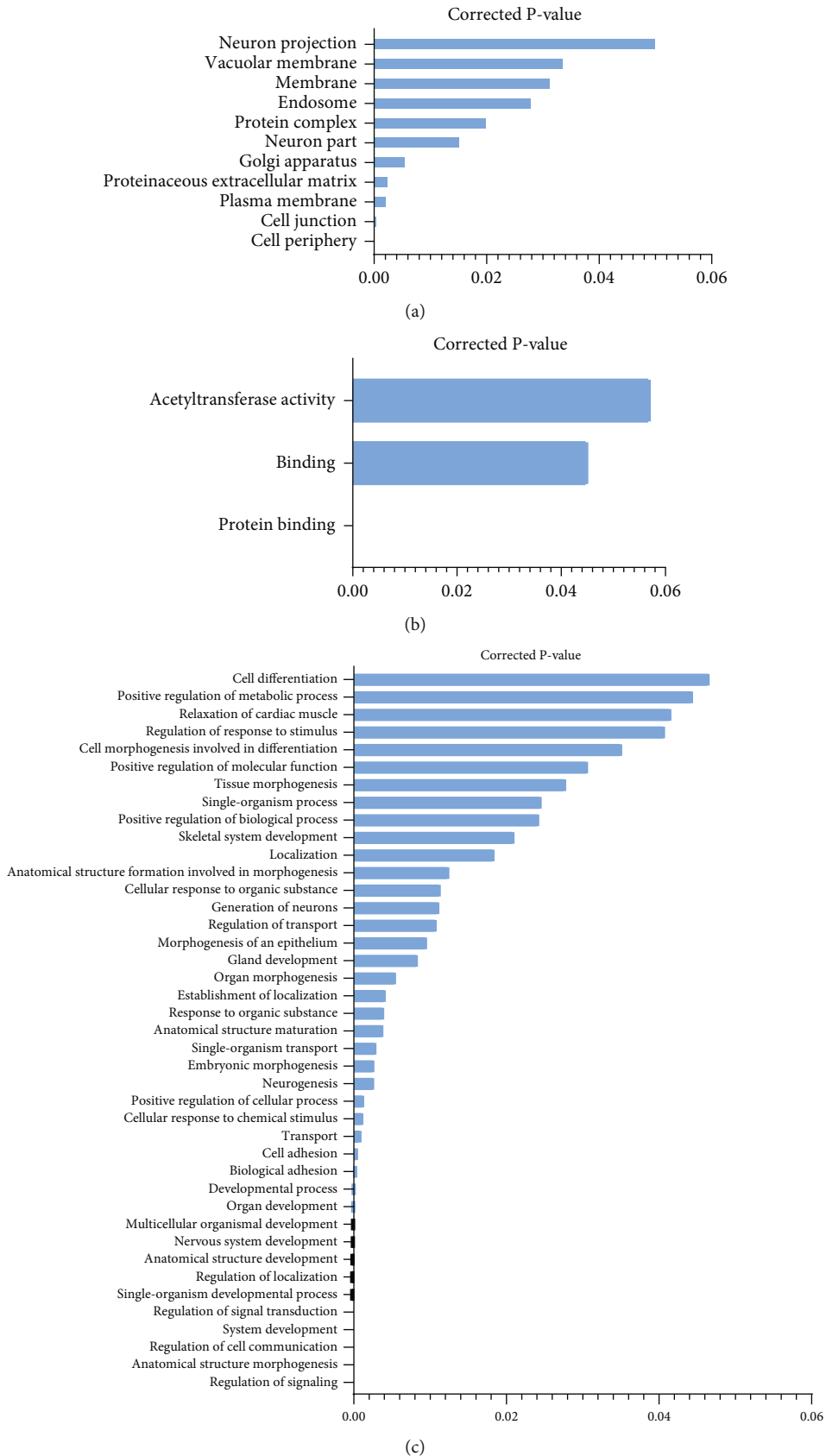


FIGURE 4: The  $p$  value of GO terms in experimental difference of the control vs. model. (a) GO analysis in cellular components. (b) GO analysis in molecular function. (c) GO analysis in biological processes (GO terms, which is significantly enriched in the target gene corresponding to differentially expressed sRNAs, is defined as  $p$  value  $\leq 0.05$ . This figure only shows the GO term with  $p$  value  $\leq 0.05$ ).

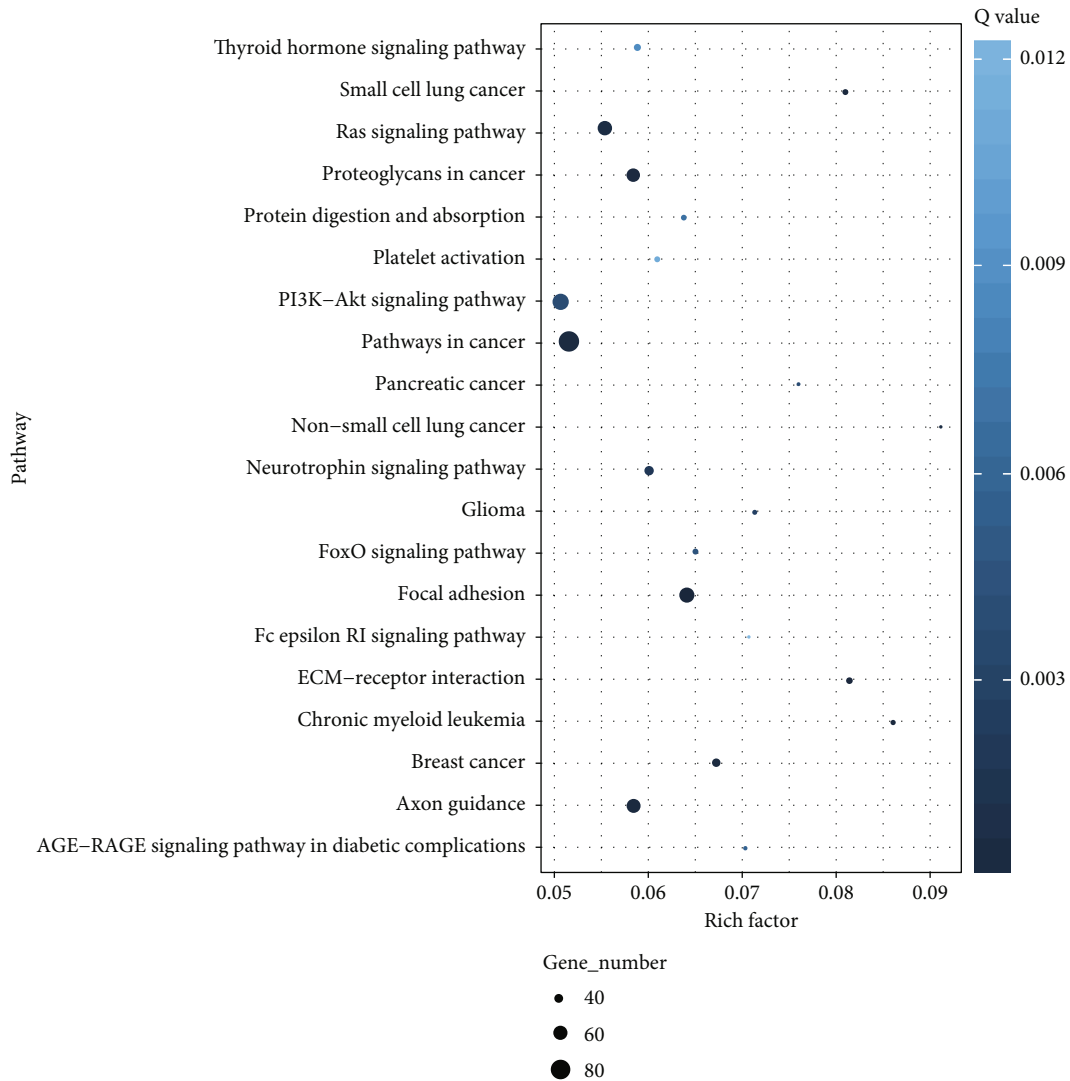


FIGURE 5: KEGG pathways of top 20 enrichment score.

the AS group were observably increased compared to the control group ( $p < 0.05$ ), respectively, while mmu-miR-107-3p showed no significant difference. mmu-miR-421-3p, mmu-miR-350-3p, and mmu-miR-184-3p in the AS group were markedly decreased compared with that in the control group ( $p < 0.05$ ), while mmu-miR-331-3p showed no significant difference. In addition, in situ hybridization assay showed that miR-146a (green) in the HFD-fed group was significantly improved than in the control group (Figure 7(b)), indicating that the level of miR-146a is closely associated with the development of atherosclerosis. These results indicated that mmu-miR-378d, mmu-miR-181b-5p, mmu-miR-146a-5p, mmu-miR-421-3p, mmu-miR-350-3p, and mmu-miR-184-3p had good consistency with the deep sequencing results, which could serve as promising noninvasive biomarkers for AS.

#### 4. Discussion

Atherogenesis was identified by the plaque area and plaque composition in aortic roots [31]. This is the first study to explore the effects of miRNA expression profiles in plasma

extracellular vesicles of LDLr<sup>-/-</sup> mice by combining two approaches, such as high-throughput sequencing and bioinformatics analyses. Our results suggested that the extracellular vesicle composition of plasma from mice with AS was far different than normal mice. The changes in plasma extracellular vesicle miRNA expression profiles may reflect the physiological and pathological processes of AS and may provide potential targets for treating AS [32].

In this study, 17 miRNAs were differentially expressed in extracellular vesicles extracted from the plasma of LDLr<sup>-/-</sup> mice and normal mice. These included 8 upregulated miRNAs and 9 downregulated miRNAs that may be involved in developing AS. Out of these 17, 8 highly expressed miRNAs (4 upregulated and 4 downregulated miRNAs) were further assessed by TaqMan-based qRT-PCR. Our results showed the most differentially expressed miRNAs (miR-378d, miR-181b-5p, miR-146a-5p, miR-421-3p, miR-350-3p, and miR-184-3p) had good consistency with the deep sequencing results. Therefore, the six plasma miRNA panels mentioned above may have a promising diagnostic biomarker potential against AS.

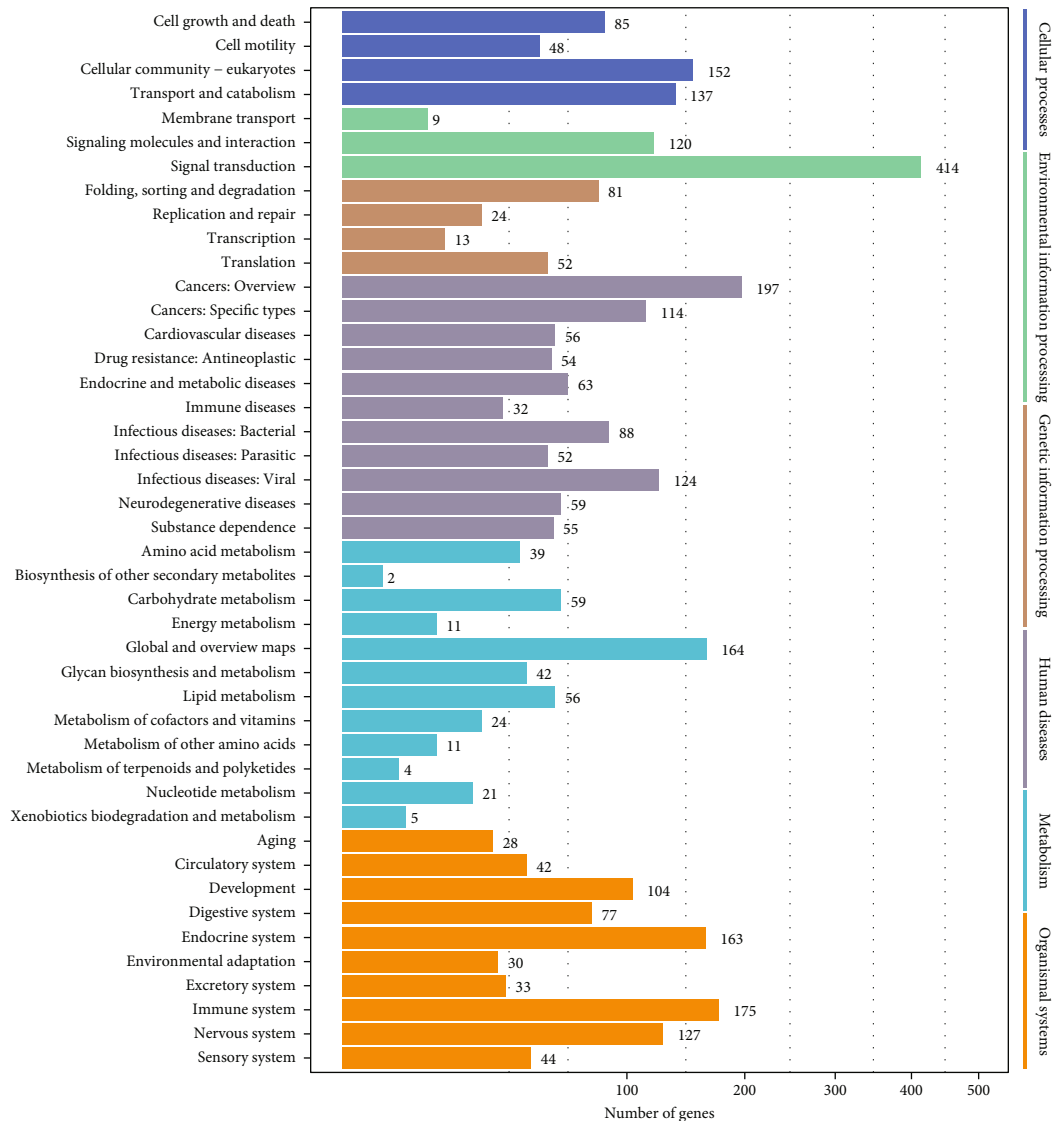


FIGURE 6: Classification statistics of KEGG channel annotation.

The literature has confirmed that circulating miRNAs can be used as potential diagnostic biomarkers and prognostic factors in various diseases including AS [33–35]. Our data indicated that the upregulation of miR-378d, miR-181b-5p, and miR-146a-5p or downregulation of miR-421-3p, miR-350-3p, and miR-184-3p were closely related to AS. miR-378 and miR-421 are endogenous negative regulators of Ras signaling and cardiac hypertrophy and regulators of mitochondrial disruption and cardiomyocyte apoptosis, respectively [36–38]. Deleting miR-378 will lead to cardiac hypertrophy, and miR-421 may be a potential therapeutic target for heart disease. The miR-181 family is a target related to endothelial cell activation and immune cell homeostasis and plays an important role in vascular inflammatory responses by controlling key signaling pathways [37]. miR-146a mediates immune response and atherosclerotic inflammation, while miR-184 is involved in adipogenesis in PKP2-deficient cells [39, 40]. miR-350-3p is a new target for treating age-related inflammatory diseases due to its impaired age-related macrophage function [41]. In

summary, atherosclerosis may be closely related to multiple biological processes that may directly or indirectly be involved in regulating the six miRNAs mentioned above.

EV miRNAs play an important role in diagnosing and treating multifactorial diseases, including T2DM and its cardiovascular complications. The collection of harvesting rare EV fractions or subpopulations increased the potential for miRNA biomarker discovery, and EV-shuttle miR-146a-5p improved its performance in detecting type 2 diabetes and its complications [42, 43]. Moreover, the inhibition of miR-1 reduced endothelial inflammation *in vitro* and attenuated atherogenesis in ApoE-deficient mice [44]. Endothelial microparticles promote vascular endothelial repair by delivering functional miR-126 into recipient cells [45]. miR-92a can be transported to macrophages through extracellular vesicles to regulate KLF4 levels, thus leading to the atheroprone phenotypes of macrophage and, hence, atherosclerotic lesion formation [46]. Endothelial microvesicle-mediated transfer of functional miR-92a-3p regulates angiogenesis in recipient

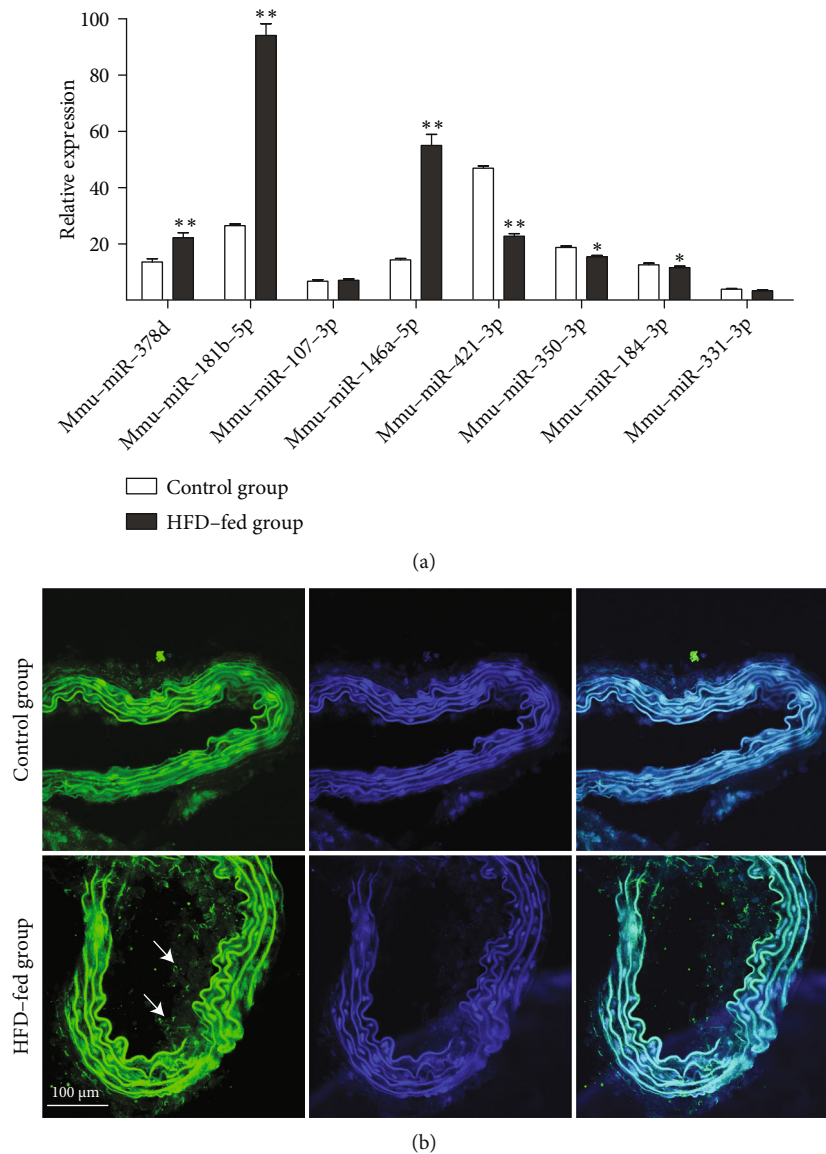


FIGURE 7: Validation of expression of miRNAs. (a) Validation by qRT-PCR. (b) The content of miR-146a in arterial tissue was evaluated by in situ hybridization from the mice. Scale bars 100  $\mu\text{m}$ . Each value represents the mean  $\pm$  SEM ( $n = 6$ ). \* $p < 0.05$ , \*\* $p < 0.01$  vs. the control group.

endothelial cells by a THBS1- (thrombospondin 1-) dependent mechanism [47].

Reverse-transcription polymerase chain reaction (RT-PCR) is a powerful combination of assays useful in detection and measurement of expressed RNA transcripts. Currently, commonly used PCR-based procedures are standard, real-time, or quantitative (qPCR or qRT-PCR), or TaqMan [48]. We choose TaqMan-based qRT-PCR in this article. U6 belongs to small nuclear RNA (snRNA) in cells. U6 is stable, abundant, highly conserved, and ubiquitous in eukaryotic cells. So, we choose U6 snRNA as an internal reference gene [27, 28].

When we analyzed the potential function of differentially expressed miRNAs using the KEGG pathway, we found that

the focal adhesion and Ras signaling pathway seemed to be strongly associated with the development of atherosclerosis [22, 49]. Adhesion of monocytes and lymphocytes to endothelium is also affected by other associated molecules inside endothelial cells [50], such as focal adhesion kinase (FAK). FAK is recruited to sites of focal adhesion (FA) and tightly linked to various structural networks of intracellular cytoskeletons and extracellular matrix (ECM) [40]. In addition, the Ras signaling pathway has been reported in the literature to participate in the cellular aging process [36]. Since Ras can mediate a variety of atherosclerotic stimuli including growth factors and oxidative stress, it is speculated that it can promote the aging of vascular cells and participate in the pathogenesis of atherosclerosis [36].

In summary, the differentially expressed genes (DEG) and related pathways that may be involved in AS in LDLr<sup>-/-</sup> mice were comprehensively analyzed by bioinformatics in this study. We found a variety of miRNAs in plasma extracellular vesicles that are closely related to the physiological and pathological processes of AS and predicted the potential functions of related pathways and the targets of miRNAs. These results will facilitate the development of biomarkers as targets for diagnosing or treating AS.

## Data Availability

The data used to support the findings of this study are included within the article. The data used to support the findings of this study are included within the supplementary information file(s).

## Additional Points

**Key Points.** (i) The atherosclerosis model had been established in LDLr<sup>-/-</sup> mice. (ii) Extracellular vesicles were isolated and identified in the plasma. (iii) Six plasma miRNA panels may serve as promising diagnostic biomarkers for AS. (iv) Circular miRNAs pave the way for biomarkers and novel targets for atherosclerosis.

## Ethical Approval

All procedures of the current study were carried out according to the criteria outlined in the “Guide for the Care and Use of Laboratory Animals” prepared by the National Academy of Sciences and published by the National Institutes of Health (NIH publication no. 85-23, revised 1996) and approved by the Ethical Committee of Suzhou University (SZU-19002).

## Conflicts of Interest

The authors declare that there are no conflicts of interest.

## Acknowledgments

This work was supported by the National Natural Science Foundation of China (82170481), Anhui Natural Science Foundation (2008085J39 and 2108085MH314), Excellent top-notch Talents Training program of Anhui Universities (gwgwfx2021038), Natural Science Foundation of Anhui Educational Committee (KJ2020A0728), State Key Laboratory for Chemistry and Molecular Engineering of Medicinal Resources (Guangxi Normal University) (CMEMR2021-B03), Excellent Young Talents Plan of Guizhou Medical University (No. 2022-104), Guizhou Provincial Key Laboratory of Pharmaceuticals, Engineering Research Center for the Development and Application of Ethnic Medicine and TCM (Ministry of Education) (YWZJ2022-03), Postdoctoral Foundation of Jiangsu Province (1601173B), and Suzhou Engineering Research Center of Natural Medicine and Functional Food (SZ2017ZX06).

## Supplementary Materials

**Supplementary 1.** Supplementary Table 1: the results of miRNA classification and annotation ( $n = 8$ ).

**Supplementary 2.** Supplementary Table 2: unknown miRNA prediction results.

**Supplementary 3.** Supplementary Table 3: target gene prediction of 17 differentially expressed miRNAs by four software (TargetScan, PITA, miRanda, and RNAhybrid).

## References

- [1] F. Wang, J. Lu, X. Peng et al., “Integrated analysis of micro-RNA regulatory network in nasopharyngeal carcinoma with deep sequencing,” *Journal of Experimental & Clinical Cancer Research*, vol. 35, no. 1, p. 17, 2016.
- [2] H.-C. Chung, V.-G. Nguyen, W.-T. Oh et al., “Inhibition of porcine endogenous retrovirus by multi-targeting micro RNA against long terminal region,” *Transplantation proceedings*, vol. 49, no. 9, pp. 2225–2232, 2017.
- [3] M. Lehtihet, H. Bhuiyan, A. Dalby, M. Ericsson, and L. Ekström, “Longitudinally monitoring of P-III-NP, IGF-I, and GH-2000 score increases the probability of detecting two weeks’ administration of low-dose recombinant growth hormone compared to GH-2000 decision limit and GH isoform test and micro RNA markers,” *Drug Testing and Analysis*, vol. 11, no. 3, pp. 411–421, 2019.
- [4] Z. Wang, L. C. Kong, B. Y. Jia et al., “Analysis of the microRNA expression profile of bovine monocyte-derived macrophages infected with Mycobacterium avium subsp. paratuberculosis reveals that miR-150 suppresses cell apoptosis by targeting PDCD4,” *International journal of molecular sciences*, vol. 20, p. 2708, 2019.
- [5] A. K. V. Beita and T. F. Whayne, “The superior mesenteric artery: from syndrome in the young to vascular atherosclerosis in the old,” *Hematological Agents*, vol. 17, no. 2, pp. 74–81, 2019.
- [6] X. Lou, X. Ma, D. Wang et al., “Systematic analysis of long non-coding RNA and mRNA expression changes in ApoE-deficient mice during atherosclerosis,” *Molecular and Cellular Biochemistry*, vol. 462, no. 1-2, pp. 61–73, 2019.
- [7] B. Trojanowicz, T. Imdahl, C. Ulrich, R. Fiedler, and M. Girndt, “Circulating miR-421 targeting leucocytic angiotensin converting enzyme 2 is elevated in patients with chronic kidney disease,” *Nephron*, vol. 141, no. 1, pp. 61–74, 2019.
- [8] M. C. Phillips, “Apolipoprotein E isoforms and lipoprotein metabolism,” *IUBMB Life*, vol. 66, no. 9, pp. 616–623, 2014.
- [9] W. Chang, F. Zhu, H. Zheng et al., “Glucagon-like peptide-1 receptor agonist dulaglutide prevents ox-LDL-induced adhesion of monocytes to human endothelial cells: an implication in the treatment of atherosclerosis,” *Molecular Immunology*, vol. 116, pp. 73–79, 2019.
- [10] J. Li, H. Xue, T. Li et al., “Exosomes derived from mesenchymal stem cells attenuate the progression of atherosclerosis in ApoE<sup>-/-</sup> mice via miR-let7 mediated infiltration and polarization of M2 macrophage,” *Biochemical and Biophysical Research Communications*, vol. 510, no. 4, pp. 565–572, 2019.
- [11] B. Laffont and K. J. Rayner, “MicroRNAs in the pathobiology and therapy of atherosclerosis,” *The Canadian Journal of Cardiology*, vol. 33, no. 3, pp. 313–324, 2017.

- [12] Y. Lu, T. Thavarajah, W. Gu, J. Cai, and Q. Xu, "Impact of miRNA in atherosclerosis," *Arteriosclerosis, Thrombosis, and Vascular Biology*, vol. 38, no. 9, pp. e159–e170, 2018.
- [13] N. P. Patil, V. Le, A. D. Sligar et al., "Algal polysaccharides as therapeutic agents for atherosclerosis," *Frontiers in Cardiovascular Medicine*, vol. 5, 2018.
- [14] S. Oppi, T. F. Lüscher, and S. Stein, "Mouse models for atherosclerosis research—which is my line?," *Frontiers in Cardiovascular Medicine*, vol. 6, 2019.
- [15] T. T. Liu, Y. Zeng, K. Tang, X. Chen, W. Zhang, and X. L. Xu, "Dihydromyricetin ameliorates atherosclerosis in LDL receptor deficient mice," *Atherosclerosis*, vol. 262, pp. 39–50, 2017.
- [16] K. F. Zhai, J. R. Zheng, Y. M. Tang et al., "The saponin D39 blocks dissociation of non-muscular myosin heavy chain IIA from TNF receptor 2, suppressing tissue factor expression and venous thrombosis," *British Journal of Pharmacology*, vol. 174, pp. 2818–2831, 2017.
- [17] C. T. Xiao, W. J. Lai, W. A. Zhu, and H. Wang, "MicroRNA derived from circulating exosomes as noninvasive biomarkers for diagnosing renal cell carcinoma," *Oncotargets and Therapy*, vol. Volume 13, pp. 10765–10774, 2020.
- [18] H. Rodriguez-Caro, R. Dragovic, M. Shen et al., "In vitro decidualisation of human endometrial stromal cells is enhanced by seminal fluid extracellular vesicles," *Journal of extracellular vesicles*, vol. 8, no. 1, p. 1565262, 2019.
- [19] C. Théry, K. W. Witwer, E. Aikawa et al., "Minimal information for studies of extracellular vesicles 2018 (MISEV2018): a position statement of the International Society for Extracellular Vesicles and update of the MISEV2014 guidelines," *Journal of extracellular vesicles*, vol. 7, no. 1, p. 1535750, 2018.
- [20] Y. Huang, J. Xiong, P. Brown, and X. Sun, "Discovery of microRNAs from *Batrachuperus yenyuanensis* using deep sequencing and prediction of their targets," *Biochemistry (Moscow)*, vol. 84, no. 4, pp. 380–389, 2019.
- [21] X. Lu, J. Wu, M. Ma, X. Wu, J. Wen, and J. Yu, "An integrated deep sequencing analysis of microRNAs in transplanted corneas," *Molecular Immunology*, vol. 101, pp. 429–439, 2018.
- [22] J. Zhou, C. Zhang, X. Wu et al., "Identification of genes and pathways related to atherosclerosis comorbidity and depressive behavior via RNA-seq and bioinformatics analysis in ApoE<sup>-/-</sup> mice," *Annals of Translational Medicine*, vol. 7, no. 23, p. 733, 2019.
- [23] H. Torkey, L. S. Heath, and M. ElHefnawi, "MicroTarget: microRNA target gene prediction approach with application to breast cancer," *Journal of Bioinformatics and Computational Biology*, vol. 15, no. 4, p. 1750013, 2017.
- [24] F. Yuan, L. Lu, Y. Zhang, S. Wang, and Y.-D. Cai, "Data mining of the cancer-related lncRNAs GO terms and KEGG pathways by using mRMR method," *Mathematical Biosciences*, vol. 304, pp. 1–8, 2018.
- [25] Z. Li, J. Wu, W. Wei et al., "Association of serum miR-186-5p with the prognosis of acute coronary syndrome patients after percutaneous coronary intervention," *Frontiers in Physiology*, vol. 10, p. 686, 2019.
- [26] H.-D. Phan, J. Li, M. Poi, and K. Nakanishi, "Quantification of miRNAs co-immunoprecipitated with Argonaute proteins using SYBR green-based qRT-PCR," *Argonaute Proteins*, pp. 29–40, 2018.
- [27] T. Hennig, A. B. Prusty, B. B. Kaufert et al., "Selective inhibition of miRNA processing by a herpesvirus-encoded miRNA," *Nature*, vol. 605, no. 7910, pp. 539–544, 2022.
- [28] K. Inoue, N. Ogonuki, S. Kamimura et al., "Loss of H3K27me3 imprinting in the Sfbmt2 miRNA cluster causes enlargement of cloned mouse placentas," *Nature Communications*, vol. 11, no. 1, p. 2150, 2020.
- [29] K. Zhai, H. Duan, W. Wang, S. Zhao, and Z. Wei, "Ginsenoside Rg1 ameliorates blood-brain barrier disruption and traumatic brain injury via attenuating macrophages derived exosomes miR-21 release," *Acta Pharmaceutica Sinica B*, vol. 11, no. 11, pp. 3493–3507, 2021.
- [30] L.-X. Yu, B.-L. Zhang, Y. Yang et al., "Exosomal microRNAs as potential biomarkers for cancer cell migration and prognosis in hepatocellular carcinoma patient-derived cell models," *Oncology Reports*, vol. 41, no. 1, pp. 257–269, 2019.
- [31] Z. Ruan, T. Chu, L. Wu et al., "miR-155 inhibits oxidized low-density lipoprotein-induced apoptosis in different cell models by targeting the p85 $\alpha$ /AKT pathway," *Journal of Physiology and Biochemistry*, vol. 76, no. 2, pp. 329–343, 2020.
- [32] A. Churov, V. Summerhill, A. Grechko, V. Orekhova, and A. Orekhov, "MicroRNAs as potential biomarkers in atherosclerosis," *International Journal of Molecular Sciences*, vol. 20, no. 22, p. 5547, 2019.
- [33] A. Q. Yu, Z. X. Wang, W. Wu, K. Y. Chen, S. R. Yan, and Z. B. Mao, "Circular RNA CircCCNB1 sponges micro RNA-449a to inhibit cellular senescence by targeting CCNE2," *Aging (Albany NY)*, vol. 11, no. 22, pp. 10220–10241, 2019.
- [34] J. Yu, Q. Xu, X. Zhang, and M. Zhu, "Circulating microRNA signatures serve as potential diagnostic biomarkers for helicobacter pylori infection," *Journal of Cellular Biochemistry*, vol. 120, no. 2, pp. 1735–1741, 2019.
- [35] M. W. Feinberg and K. J. Moore, "MicroRNA regulation of atherosclerosis," *Circulation Research*, vol. 118, no. 4, pp. 703–720, 2016.
- [36] T. Minamino, T. Yoshida, K. Tateno et al., "Ras induces vascular smooth muscle cell senescence and inflammation in human atherosclerosis," *Circulation*, vol. 108, no. 18, pp. 2264–2269, 2003.
- [37] X. Sun, A. Sit, and M. W. Feinberg, "Role of miR-181 family in regulating vascular inflammation and immunity," *Trends in Cardiovascular Medicine*, vol. 24, no. 3, pp. 105–112, 2014.
- [38] M. Lu, S. Yuan, S. Li, L. Li, M. Liu, and S. Wan, "The exosome-derived biomarker in atherosclerosis and its clinical application," *Journal of Cardiovascular Translational Research*, vol. 12, no. 1, pp. 68–74, 2019.
- [39] P. Gurha, X. Chen, R. Lombardi, J. T. Willerson, and A. J. Marian, "Knockdown of plakophilin 2 downregulates miR-184 through CpG hypermethylation and suppression of the E2F1 pathway and leads to enhanced adipogenesis in vitro," *Circulation Research*, vol. 119, no. 6, pp. 731–750, 2016.
- [40] Y. Seo, J. Park, W. Choi et al., "Antiatherogenic effect of resveratrol attributed to decreased expression of ICAM-1 (intercellular adhesion molecule-1)," *Arteriosclerosis, Thrombosis, and Vascular Biology*, vol. 39, no. 4, pp. 675–684, 2019.
- [41] H. Chang, X. Wang, and S. Yang, "miR-350-3p contributes to age-associated impairment of IL-6 production by macrophages," *Immunological Investigations*, vol. 47, no. 8, pp. 790–800, 2018.
- [42] F. Prattichizzo, G. Maccacchione, A. Giuliani et al., "Extracellular vesicle-shuttled miRNAs: a critical appraisal of their potential as nano-diagnostics and nano-therapeutics in type 2 diabetes mellitus and its cardiovascular complications," *Theranostics*, vol. 11, no. 3, pp. 1031–1045, 2021.

- [43] F. Prattichizzo, V. De Nigris, J. Sabbatinelli et al., “CD31+ extracellular vesicles from patients with type 2 diabetes shuttle a miRNA signature associated with cardiovascular complications,” *Diabetes*, vol. 70, no. 1, pp. 240–254, 2021.
- [44] F. Jiang, Q. Chen, W. Wang, Y. Ling, Y. Yan, and P. Xia, “Hepatocyte-derived extracellular vesicles promote endothelial inflammation and atherogenesis via microRNA-1,” *Journal of Hepatology*, vol. 72, no. 1, pp. 156–166, 2020.
- [45] F. Jansen, X. Yang, M. Hoelscher et al., “Endothelial microparticle-mediated transfer of microRNA-126 promotes vascular endothelial cell repair via SPRED1 and is abrogated in glucose-damaged endothelial microparticles,” *Circulation*, vol. 128, no. 18, pp. 2026–2038, 2013.
- [46] Y. J. Chang, Y. S. Li, C. C. Wu et al., “Extracellular microRNA-92a mediates endothelial cell-macrophage communication,” *Arteriosclerosis, Thrombosis, and Vascular Biology*, vol. 39, no. 12, pp. 2492–2504, 2019.
- [47] Y. Liu, Q. Li, M. R. Hosen et al., “Atherosclerotic conditions promote the packaging of functional microRNA-92a-3p into endothelial microvesicles,” *Circulation Research*, vol. 124, no. 4, pp. 575–587, 2019.
- [48] J. Elfman and H. Li, “Detection and measurement of chimeric RNAs by RT-PCR,” *Methods in Molecular Biology*, vol. 2079, pp. 83–94, 2020.
- [49] P. Wang, H. Ma, Y. Zhang et al., “Plasma exosome-derived microRNAs as novel biomarkers of traumatic brain injury in rats,” *International Journal of Medical Sciences*, vol. 17, no. 4, pp. 437–448, 2020.
- [50] X. Xu, L. Tian, and Z. Zhang, “Triptolide inhibits angiogenesis in microvascular endothelial cells through regulation of miR-92a,” *Journal of physiology and biochemistry*, vol. 75, no. 4, pp. 573–583, 2019.